Scientific paper

Electrolyte Rejection from Charged Nanoporous Material†

Miha Lukšič, Barbara Hribar-Lee and Vojko Vlachy*

Faculty of Chemistry and Chemical Technology, University of Ljubljana, Aškerčeva c. 5, SI-1000 Ljubljana, Slovenia

** Corresponding author: e-mail: vojko.vlachy@fkkt.uni-lj.si*

Received: 07-06-2007

†Dedicated to Prof. Dr. Jože Škerjanc on the occasion of his 70th birthday

Abstract

Adsorption of the charge and size symmetric +1 : –1 primitive model electrolyte in disordered media (matrix) with charged (or neutral) obstacles was studied using the Replica Ornstein-Zernike theory and Grand Canonical Monte Carlo computer simulation. The charged matrix was prepared by a rapid quench of the +1 : z_-^0 (z_-^0 = –1, –2, –3, and –4) electrolyte solution being in equilibrium at temperature T_0, and relative permittivity ε_0. Than the positive ions were allowed to anneal and mix with the invading +1 : –1 electrolyte at T, ε_1, while the anions were left quenched and represented the collection of obstacles, called here matrix, to which the external electrolyte was adsorbed. To complement the data for charged adsorbent we also considered the adsorption of the same +1 : –1 electrolyte in the matrix prepared from hard sphere fluid and in the electroneutral matrix formed by quenched +1:–1 electrolyte. In the latter case, the (electroneutral) matrix was represented as an equilibrium distribution (T_0, ε_0) of monovalent cations and anions being quenched during the adsorption of an invading model electrolyte. Special attention was paid to the thermodynamic properties of the adsorbed fluid. We were particularly interested in the mean activity coefficient of the adsorbed electrolyte and in the Donnan exclusion coefficient as a function of the charge density of the matrix. At higher concentrations of the invading electrolyte the adsorption was dominated by the excluded volume effect of the matrix, whereas at low electrolyte concentrations the adsorption was governed by the combined effect of the matrix charge density and the excluded volume. These findings are in good qualitative agreement with those obtained previously for the electrolyte adsorbed in charged cylindrical micropores.

Keywords: Disordered charged matrix, adsorption, Donnan equilibrium, electrolyte, replica Ornstein-Zernike equation, Grand Canonical Monte Carlo simulation

1. Introduction

The partitioning of ions between a porous phase and a bulk solution finds its practical application in many industrial, technological, and analytical processes. Ion separation and/or ion-exchange, desalination of water, chemistry of gels, are just few of such examples. Accordingly, it is important to develop and test the theories, which can predict the behaviour of the system for different model parameters. Heterogeneous systems containing ions were, because of their importance for science an technology, the subject of many theoretical and experimental studies (see for example 1–6). The phenomenon of ion partitioning has often been treated as the classical Donnan equilibrium.[7] Due to the charged groups present in the porous material there is an excess of counterions next to the matrix particles, while the co-ions are most often excluded from this region. This results in the overall exclusion of the electrolyte from the charged microporous material. As a convenient measure of the exclusion effect, the Donnan exclusion coefficient, Γ, is defined as:

$$\Gamma = \frac{c_{bulk} - c_-^1}{c_{bulk}} \tag{1}$$

In last decades, a new class of theories appeared in which the disordered porous material filled with fluid is treated as a partly quenched system in which some of the degrees of freedom are quenched and others are annealed. The system differs from a regular mixture; the statistical-mechanical average needed to obtain the free energy derivatives of the confined fluid becomes a double ensemble average.[8–16] The thermodynamic and structural properties of these systems can be obtained from computer simulations and, the so called, replica integral equation theory. The present work is a continuation of our studies of partly quenched systems containing charges,[17–24] however, it differs from these works in one important aspect. The quenc-

hed "phase" (we shall call it also the *matrix*) is not electroneutral, but rather represented by a distribution of negatively charged ions being "frozen" (quenched) in their equilibrium positions. Within such a matrix the model +1 : –1 electrolyte, with an excess of counterions (ions of the opposite charge sign as the matrix particles) to maintain the electroneutrality, is distributed. The adsorbed electrolyte is in thermodynamic equilibrium with the surrounding bulk solution of the same chemical composition. The overall system is therefore electroneutral but the two subsystems, containing either quenched or annealed particles, are not. The model used here was in detail described in our recent paper,[25] hereafter called **I**, where the relevant theoretical expressions were outlined.

In this article we present the results for the thermodynamic properties such as the mean activity coefficient, the excess internal energy, and the isothermal compressibility of a restricted primitive model +1 : –1 electrolyte confined in matrices composed of ionic obstacles with valencies $z_-^0 = -1, -2, -3$, and –4. The net charge of a particular matrix depended therefore on the valence of the obstacles as also on their concentration. It has been shown before[2] that Donnan coefficient, Γ, of the +1 : –1 electrolyte in charged cylindrical micropores increases with the increasing pore charge density (in ion-exchange literature called also capacity of matrix), depending on the radius of the capillary. In the present work we were interested in how the concentration of obstacles and their charge (valence) influence the Donnan exclusion coefficient and the related quantity, the mean activity of the confined electrolyte. To complement the picture, and to show more clearly the differences arising due to the net charge of the matrix, we also show some results for the adsorption of the +1 : –1 electrolyte in uncharged hard-sphere matrices ($z^0 = 0$), and in electroneutral matrices formed of an equal number of cations and anions ($z_+^0 = |z_-^0| = 1$).

2. The Model and Methods

The model used here was the same as described in **I**. The system studied consisted of two subsystems: one was composed of the quenched and the other of the annealed particles. The modelled system was considered on a McMillan-Mayer level of description; the solvent was treated implicitly and therefore characterized only via its dielectric constant. The matrix was prepared by a rapid quench of the +1 : –1, +1 : –2, +1 :–3, and +1: –4 electrolyte solutions being in equilibrium at temperature T_0 and with the dielectric constant of the solvent, ε_0. The equilibrium distribution was assumed to be preserved during this procedure. After the quench, the positive ions were allowed to anneal and mix with the invading +1 : –1 electrolyte, while the quenched anions represented the matrix (adsorbent).

The annealed subsystem was modelled as a restricted primitive model +1 : –1 electrolyte in thermodynamic equilibrium with the matrix particles at the temperature of observation T and dielectric constant of the media being ε_1. The system was electroneutral as a whole: there was an equivalent number of positively charged ions of the annealed electrolyte to compensate the negative charge of the matrix. As in previous studies, it was supposed that the annealed "phase" could not affect the distribution of (frozen) matrix particles. The ions were modelled as charged hard spheres of equal size ($\sigma_+^0 = \sigma_-^0 = \sigma_+^1 = \sigma_-^1 =$ 4.25 Å), interacting through the pair potentials:

$$U_{ij}^{00}(r) = \begin{cases} \infty & r < (\sigma_i^0 + \sigma_j^0)/2 \\ \dfrac{z_i^0 z_j^0 \lambda_{B,0}}{\beta_0} \cdot \dfrac{1}{r} & r \geq (\sigma_i^0 + \sigma_j^0)/2 \end{cases} \quad (2)$$

$$U_{ij}^{10}(r) = \begin{cases} \infty & r < (\sigma_i^1 + \sigma_j^0)/2 \\ \dfrac{z_i^1 z_j^0 \lambda_{B,1}}{\beta_1} \cdot \dfrac{1}{r} & r \geq (\sigma_i^1 + \sigma_j^0)/2 \end{cases} \quad (3)$$

and

$$U_{ij}^{11}(r) = \begin{cases} \infty & r < (\sigma_i^1 + \sigma_j^1)/2 \\ \dfrac{z_i^1 z_j^1 \lambda_{B,1}}{\beta_1} \cdot \dfrac{1}{r} & r \geq (\sigma_i^1 + \sigma_j^1)/2 \end{cases} \quad (4)$$

The indices 0 denote the matrix components and the annealed ions bear indices 1. As usual, the sign "+" denotes cations, the sign "–" stands for anions (note that for charged matrix j in equation 3 can only be "–"), $\lambda_{B,0}$ and $\lambda_{B,1}$ are the Bjerrum lengths of the matrix and fluid respectively: $\lambda_{B,0} = e^2/(4\pi\varepsilon_0\varepsilon k_B T_0)$, and $\lambda_{B,1} = e^2/(4\pi\varepsilon_1\varepsilon k_B T)$. Further, $\beta = 1/(k_B T)$, where k_B is the Boltzmann constant, and the ε_0 and ε_1 are the dielectric constants at the respective temperatures, ε being here the permittivity of vacuum. In the present work, the temperature of a quench, T_0, was the same as the temperature of the observation, T = 298 K, and $\varepsilon_0 = \varepsilon_1 = 78.4$. For aqueous solutions this resulted in $\lambda_{B,0} = \lambda_{B,1} = 7.14$ Å. This system was studied using the replica Ornstein-Zernike (ROZ) theory, supplemented by the hypernetted-chain (HNC) closure approximation. In few cases also the Grand Canonical Monte Carlo computer simulation method was used to test the validity of the theoretical results.

In addition to above, we also prepared the (*i*) hard-sphere matrices and (*ii*) electroneutral ionic matrices. In case (*i*) the matrix was taken to be a representative equilibrium distribution of uncharged hard spheres ($\sigma^0 = 4.25$ Å, $z^0 = 0$). In example (*ii*) an equilibrium distribution of charge and size symmetric cations and anions ($\sigma_+^0 = \sigma_-^0 = 4.25$ Å, $z_+^0 = |z_-^0| = +1$), corresponding to T_0 and ε_0 was assumed to be the matrix. Within such matrices, (*i*) and (*ii*), the +1 : –1 electrolyte as characterized above was allowed to equilibrate at conditions T and ε_1 (for more details see our previous studies 23 and **I**).

2. 1. The Replica Ornstein-Zernike Theory

The replica Ornstein-Zernike equations, which apply to the model at hand, were in detail described in **I**. The distribution of matrix particles obtained in terms of the pair correlation functions follows from the first integral equation:

$$\mathbf{H}^{00} - \mathbf{C}^{00} = \mathbf{C}^{00} \otimes \rho^0 \mathbf{H}^{00} \tag{5}$$

where ρ^0 is a 2 × 2 diagonal matrix with diagonal elements $\rho^0_+ = \rho^0_-$, and the symbol ⊗ denotes convolution. The correlation functions H^{00} and C^{00} in equation (5) are 2 × 2 symmetric matrices with the elements $f^{00}_{--}(r) = f^{00}_{++}(r)$; $f^{00}_{+-}(r) = f^{00}_{-+}(r)$, where *f* stands for *h* or *c*.

Next we present the ROZ equations for the fluid-matrix and fluid-fluid correlations. Here the matrix cations are treated as a template for the matrix denoted by indices 0'; the formalism for such a case was developed in Refs. 26–31. The relevant equations as given in **I** read:

$$h^{10}_{i0} - c^{10}_{i0} = c^{10}_{i0} \otimes \rho^0 h^{00}_{00} + c^{10'}_{i0'} \otimes \rho^{0'} h^{0'0}_{0'0}$$

$$+c^{11}_{ii} \otimes \rho^1_i h^{10}_{i0} + c^{11}_{ij} \otimes \rho^1_j h^{10}_{j0} - c^{12}_{ii} \otimes \rho^1_i h^{10}_{i0} - c^{12}_{ij} \otimes \rho^1_j h^{10}_{j0},$$

$$h^{10'}_{i0'} - c^{10'}_{i0'} = c^{10}_{i0} \otimes \rho^0 h^{00'}_{00'} + c^{10'}_{i0'} \otimes \rho^{0'} h^{0'0'}_{0'0'}$$

$$+c^{11}_{ii} \otimes \rho^1_i h^{10'}_{i0'} + c^{11}_{ij} \otimes \rho^1_j h^{10'}_{j0'} - c^{12}_{ii} \otimes \rho^1_i h^{10'}_{i0'} - c^{12}_{ij} \otimes \rho^1_j h^{10'}_{j0'},$$

$$h^{11}_{ij} - c^{11}_{ij} = c^{10}_{i0} \otimes \rho^0 h^{01}_{0j} + c^{10'}_{i0'} \otimes \rho^{0'} h^{0'1}_{0'j} + c^{11}_{ii} \otimes \rho^1_i h^{11}_{ij} + c^{11}_{ij} \otimes \rho^1_j h^{11}_{jj}$$

$$-c^{12}_{ii} \otimes \rho^1_i h^{21}_{ij} - c^{12}_{ij} \otimes \rho^1_j h^{21}_{jj},$$

$$h^{12}_{ij} - c^{12}_{ij} = c^{10}_{i0} \otimes \rho^0 h^{01}_{0j} + c^{10'}_{i0'} \otimes \rho^{0'} h^{0'1}_{0'j} + c^{11}_{ii} \otimes \rho^1_i h^{12}_{ij} + c^{11}_{ij} \otimes \rho^1_j h^{12}_{jj}$$

$$+c^{12}_{ii} \otimes \rho^1_i h^{11}_{ij} + c^{12}_{ij} \otimes \rho^1_j h^{11}_{jj} - 2c^{12}_{ii} \otimes \rho^1_i h^{21}_{ij} - 2c^{12}_{ij} \otimes \rho^1_j h^{21}_{jj}, \tag{6}$$

where, *i* and *j* stand for + and –, respectively. Note that although the annealed fluid is a symmetric +1 : –1 electrolyte, ρ^1_+ is not equal to ρ^1_-. The former concentration namely contains also the contribution from the annealed ions of the matrix.

The set of integral equations presented first in **I** was solved using the hypernetted-chain (HNC) closure approximation:

$$c^{mn} = \exp[-\beta U^{mn} + \gamma^{mn}] - 1 - \gamma^{mn},$$

$$c^{12} = \exp[\gamma^{12}] - 1 - \gamma^{12}, \tag{7}$$

$$c^{10'} = \exp[\gamma^{10'}] - 1 - \gamma^{10'},$$

where $\gamma^{mn} = h^{mn} - c^{mn}$, and the superscripts *m, n* take values 0, 0', and 1. A direct iteration on a grid of 16,384 points with Δr = 0.05 Å was used to solve the set of integral equations given in expressions 5–7. The relevant equation to calculate the single ion activity coefficient γ^1_i in the replica approximation reads:[25]

$$\ln \gamma^1_i = -\rho^0_- \mathbf{c}^{10}_{(s)i-}(0) - \rho^{0'}_+ \mathbf{c}^{10'}_{(s)i+}(0) - \sum_{j=+,-} \rho^1_j [\mathbf{c}^{11}_{(s)ij}(0) - \mathbf{c}^{12}_{(s)ij}(0)] +$$

$$+0.5\rho^0_- \int d\mathbf{r} h^{10}_{i-}(h^{10}_{i-} - c^{10}_{i-}) + 0.5\rho^{0'}_+ \int d\mathbf{r} h^{10'}_{i+}(h^{10'}_{i+} - c^{10'}_{i+})$$

$$+0.5 \sum_{j=+,-} \rho^1_j \int d\mathbf{r} [h^{11}_{ij}(h^{11}_{ij} - c^{11}_{ij}) - h^{12}_{ij}(h^{12}_{ij} - c^{12}_{ij})]. \tag{8}$$

where $c_s(r)$ denotes the short-range part of the direct correlation function. For the symmetric +1 : –1 electrolyte we obtained the mean activity coefficient from $\sqrt{\gamma^1_+ \gamma^1_-} = \gamma^1_\pm$. The ROZ integral equations which apply to uncharged hard sphere matrices and electroneutral ionic matrices were presented in our previous papers, see Refs. 18 and 19, respectively.

2. 2. The Grand Canonical Monte Carlo Simulation

The Grand Canonical Monte Carlo (GCMC) method enables one to calculate the equilibrium number of particles <*N*> in the observed volume *V* at a given temperature *T*, and at the chemical potential dictated by an external reservoir of particles.[32] The simulation algorithm consist of two steps: (*i*) the usual Metropolis canonical scheme, and (*ii*) the Grand Canonical part, where an electroneutral combination of ions (one cation and one anion in the case of the + 1: –1 electrolyte) is randomly inserted/removed into/from a simulation cell. The inserted and removed pair are chosen randomly. For simulation details refer to **I**.

In equations 9–11 given next, $a^1_\pm$ and $a^{bulk}_\pm$ are the mean electrolyte activities of the confined and of the bulk electrolyte, respectively. Furthermore, c^1_- and c^1_+ are the average concentrations of anions and cations within the quenched "phase", while c^{bulk}_1 is the bulk concentration at $a^{bulk}_\pm$. To calculate the mean activity coefficient of the adsorbed electrolyte, $\gamma^{bulk}_\pm$, using the equilibrium condition

$$a^1_\pm = a^{bulk}_\pm, \tag{9}$$

where

$$a^1_\pm = \gamma^1_\pm \sqrt{c^1_- c^1_+}, \tag{10}$$

and

$$a^{bulk}_\pm = \gamma^{bulk}_\pm c^{bulk}_1 \tag{11}$$

$\gamma^{bulk}_\pm$ has to be known in advance. This part of calculus was done by using the hypernetted-chain (HNC) theory (see

for example, Ref. 33), which provides accurate results for symmetric bulk electrolytes.

The matrix was prepared in a separate canonical simulation with 500 anions of valence $z_-^0 = -1$, –2 or –3, and an equivalent number of monovalent cations ($z_+^0 = +1$), distributed in a volume corresponding to the concentration equal to 0.05 M, and in case of monovalent matrix ions $z_-^0 = -1$, also to 0.5 M, 1.0 M, and 2.0 M. The equilibrium distribution was taken as the last accepted configuration after from 3 to 50×10^6 of trial moves. The coordinates of the anions, which were from now on considered to be fixed, were stored as matrix coordinates. The cations were than allowed to move freely in equilibrium with the +1 : –1 electrolyte being introduced during the Grand Canonical step. Such an open system needed first to be equilibrated over 1 to 3×10^6 GCMC moves. The production run, during which the averages were collected, required up to 5×10^8 Monte Carlo steps. The principal result of the simulation was the average concentration of the invading electrolyte, from which the Donnan coefficient (see equation 1) could be calculated.

For partly-quenched systems it is also necessary to calculate the second average: this time over all the possible realizations (distributions of obstacles) of matrix material. From previous studies we learned that, for large enough number of particles forming the matrix, only few matrix realizations were needed to obtain good statistics.[23,25] The differences between the results obtained for different equilibrium distributions of obstacles were, for the same values of other parameters, within statistical uncertainties of a single calculation. For example, for the mean activity coefficients these differences were smaller than 0.1%. For this reason the averages over annealed electrolyte were calculated for two different equilibrium distribution of the matrix particles only in the cases of 0.5 and 1.0 M matrix ($z_-^0 = -1$). In all other examples the results shown here apply to only one matrix representation. To account for the long-range forces the minimum image method, found accurate enough in previous calculations of similarly strongly coupled systems,[23] was used. In the case of the hard-sphere and electroneutral ionic matrices the procedure was similar.

3. Results and Discussion

The adsorption of +1 : –1 electrolyte ($\sigma_+^1 = \sigma_-^1 = 4.25$ Å) was studied at conditions $T = 298$ K and $\varepsilon_1 = 78.4$. The matrix particles were (*a*) uncharged hard spheres ($z^0 = 0$, $\sigma^0 = 4.25$ Å); (*b*) quenched +1 : –1 hard sphere electrolyte ($\sigma_+^0 = \sigma_-^0 = 4.25$ Å); and (*c*) hard sphere anions of valence ($z_-^0 = -1$, –2, –3 and –4 ($\sigma_-^0 = 4.25$ Å). The conditions of matrix preparation and those at which the adsorption took place were set equal, namely $\lambda_{B,0} = \lambda_{B,1} = 7.14$ Å in all the cases, except for uncharged hard sphere matrix where $\lambda_{B,0} = 0$. In all the figures, with an exception of Figure 6, the lines represent the data obtained by the ROZ/HNC theory, while the symbols denote the simulation results.

In Figure 1 we show the results for the mean activity coefficient (panel 1a), the excess internal energy (1b), and the isothermal compressibility (1c) as a function of the confined annealed electrolyte concentration, c_-^1, for different matrices.

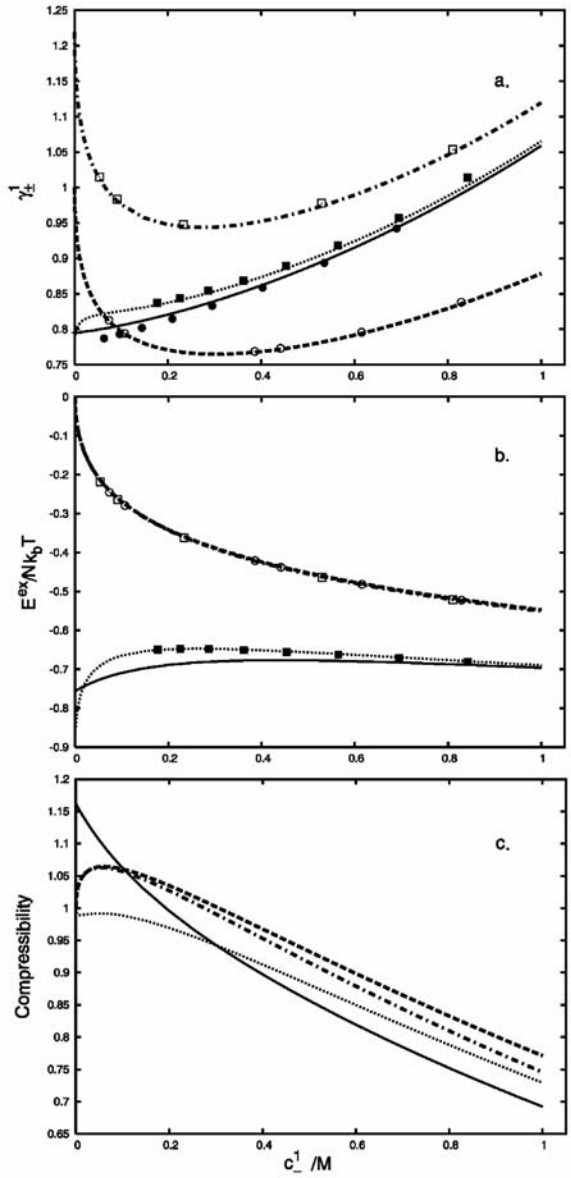

Figure 1: Thermodynamic quantities as a function of the annealed electrolyte concentration for various quenched environments. Lines denote the ROZ/HNC results, while symbols apply to the GCMC data. **a**) The mean activity coefficient: (*i*) uncharged hard sphere matrix – dash-dotted line, open squares; (*ii*) electroneutral ionic matrix ($|z_-^0| = z_+^0 = 1$, $\lambda_{B,0} = 7.14$ Å) – dotted line, full squares; (*iii*) charged matrix ($z_-^0 = -1$, $\lambda_{B,0} = 7.14$ Å) – continuous line, full circles; (*iv*) bulk electrolyte – dashed line, open circles; **b**) The excess internal energy: labelled as on panel *a* (simulation results for the case (*iii*) are not shown). **c**) The isothermal compressibility: labelled as on panel *a* (simulation results are not shown). The matrix concentration was for uncharged hard sphere matrix (*i*) $c_0 = 1.0$ M, and for electroneutral (*ii*) and charged (*iii*) matrix $c_0 = 0.5$ M. In all the cases $\lambda_{B,1} = 7.14$ Å.

We begin the discussion by presenting, from top to bottom on panel 1a, the mean activity coefficient: (*i*) for hard-sphere matrix – dash-dotted line, open squares; (*ii*) for electroneutral ionic matrix – dotted line, filled squares; (*iii*) for charged matrix ($z_-^0 = -1$) – continuous line, filled circles; and (*iv*) the mean activity coefficient for the bulk electrolyte – dashed line, open circles. The concentration of electroneutral and charged matrices (*ii* and *iii*) was $c_0 =$ 0.5 M, whereas to assure for the same packing fraction, the concentration of the uncharged hard sphere matrix (*i*) was 1.0 M. Substantial qualitative and quantitative differences between the various curves can be seen in Figure 1. For electrolyte concentrations larger than the matrix concentration, however, all the thermodynamic properties seem to follow the trend of the bulk electrolyte (dashed line).

In panel 1a we see, that the presence of uncharged hard spheres does not change the shape of the $\gamma_\pm^1$ curve even for low concentration of the invading electrolyte. The calculated values of the mean activity coefficient of electrolyte being adsorbed in such a matrix are merely shifted toward higher values, all for approximately the same amount. This seems to reflect the effect of the 'missing' volume being excluded by the matrix particles.

The other two curves in Figure 1a belong to the adsorbent containing charged obstacles and they differ qualitatively from those discussed above. The mean activity coefficient of the adsorbed electrolyte is in both cases far from the ideal and well below the bulk value. This is especially true for low values of c_-^1; this is also the region where the shapes of the two $\gamma_\pm^1$ functions differ from each other more notably. Note again that the data denoted by filled squares apply to the (*ii*), matrix with the net charge zero (electroneutral matrix), and the results shown by filled circles (lower values of the mean activity coefficient) to (*iii*) the charged matrix with volume charge density $\rho_e = -0.482 \times 10^4$ As dm^{-3}. This difference stems from the fact that the invading ions find themselves in two very different environments: in the case of the matrix composed of only negative charges, the anions are quite strongly repelled by the matrix. In any case, the repulsion is stronger than for the matrix formed by an electroneutral combination of quenched cations and anions. For a detailed discussion about the difference between the two examples the reader is referred to our previous studies, see **I** p. 5972 and the discussion in Ref. 24.

From the panel 1b we see that uncharged obstacles at this concentration, as expected, do not affect the excess internal energy of the adsorbed electrolyte. The other numerical results presented in this panel indicate that the excess energies of the electrolyte adsorbed in a charged and in an electroneutral matrix are both lower than that of the bulk electrolyte. None of the two energies approach zero for $c_-^1 \to 0$, reflecting strong interaction between ions in this limit. An explanation why the GCMC results for charged matrices are not given here is needed. Due to the different procedures of calculating the energy, i.e. in the GCMC calculation this is a summation of the pair potential and in the case of the ROZ/HNC theory integration, there is an extra term contained in the ROZ/HNC energy result. This precludes a comparison of the absolute values of the energies obtained for charged matrices (there is no such problem for electroneutral matrix) by these two methods.

The ROZ compressibility calculation shown in Figure 1c, unfortunately we do not have reliable simulation data to test the validity of the theory, are also quite interesting. The isothermal compressibility is for higher concentrations c_-^1 decreased below the bulk value. This reflects an effect of the excluded volume. The two curves with the maximum belong to the bulk electrolyte (upper curve) and to the electrolyte within hard-sphere matrix (lower curve). The maximum can be attributed to the net attraction between the various charged species and has been noticed before.[33] Values for the isothermal compressibility (Figure 1c) are for higher concentrations, c_-^1, larger for the electrolyte in electroneutral matrix, yet always lower than the values for the bulk or for the uncharged hard sphere matrix. An interesting feature of the compressibility results is that the charged and uncharged matrix cases give very different results in the limit of the small electrolyte concentration. For the former case, shown by the continuous line, the isothermal compressibility does not approach the value 1. We shall stress here that in principle the compressibility can be obtained from the GCMC simulations via the particle number fluctuations. This quantity, however, requires very long simulations to obtain reliable statistics. The results we got for this quantity from simulations were not precise enough to serve as benchmarks for the ROZ theory.

In the previous studies we showed that thermodynamic properties of an adsorbed electrolyte depend on various experimental parameters as, for example, concentrations of all components. In the next paragraph we will therefore show how the variation of the matrix concentration (charged matrix with $z_-^0 = -1$), affects the results for the mean activity coefficient, the excess internal energy, and the isothermal compressibility. These results are for four different c_-^0 values shown in Figure 2 as functions of the electrolyte concentration, c_-^1. For the excess internal energies and isothermal compresibilities, again, only the ROZ/HNC results are given, the reasons being the same as discussed for Figure 1.

Again we first discuss the mean activity coefficient results. The matrix concentrations c_-^0 are (panel 2a from top to bottom) 2.0 M (dash-dotted line, open squares); 1.0 M (dotted line, filled squares); 0.5 M (dashed line, open circles); and 0.05 M (continuous line, filled circles). The trends of the curves are similar as observed previously for the electrolyte in the electroneutral matrix.[18] The mean activity coefficient is the highest for the most concentrated matrix (dash-dotted line, open squares), and approximately follows the trend 2.0 M > 1.0 M > 0.5 M > 0.05 M. For low

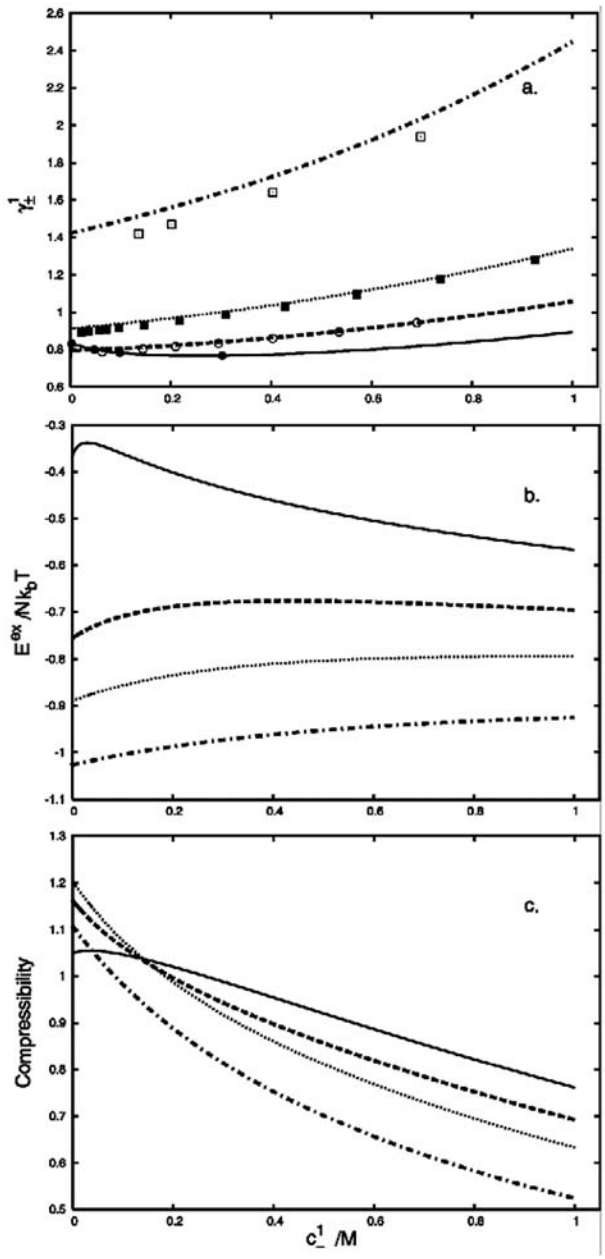

Figure 2: Thermodynamic quantities as a function of the annealed electrolyte concentration for various densities of charged matrices ($z_{-}^{0} = -1$). Lines denote ROZ/HNC results, while symbols apply for GCMC. **a**) The mean activity coefficient: (*i*) $c_0 = 0.05$ M (continuous line, full circles); (*ii*) $c_0 = 0.5$ M (dashed line, open circles); (*iii*) $c_0 = 1.0$ M (dotted line, full squares); (*iv*) $c_0 = 2.0$ M (dash-dotted line, open squares). **b**) The excess internal energy: labelled as on panel *a* (simulation results are not shown). **c**) The isothermal compressibility: labelled as on panel *a* (simulation results are not shown). In all the cases $\lambda_{B,0} = \lambda_{B,1} = 7.14$ Å.

electrolyte concentrations the $\gamma_{\pm}^{1}$ values, as calculated for $c_0 = 0.05$ M (continuous line) are slightly higher than at $c_0 = 0.5$ M (dashed line). In other cases we observed no crossover behaviour. For the most concentrated matrix ($c_0 = 2.0$ M) studied here, the computer simulation predicts somewhat lower values of $\gamma_{\pm}^{1}$ than the ROZ theory.

The excess internal energy (Figure 2b) is for $c_0 = 2.0$ M, and 1.0 M matrices an increasing function of the electrolyte concentration c_{-}^{1}, and is the lowest in the case of the most concentrated matrix. For $c_0 = 0.05$ M the situation seems to be (at a first glance) different than in other three cases. For $c_{-}^{1} < \approx 0.05$ M the energy increases, and for higher values of the electrolyte concentration decreases with the increasing c_{-}^{1}. A weakly pronounced maximum is also observed for the matrix concentration $c_0 = 0.5$ M. It could be speculated that the similar trend (decrease in the excess internal energy after c_{-}^{1} exceeds c_0) would also be observed for higher matrix concentrations if the investigated range would substantially exceed the concentration of the matrix $c_{-}^{1} >> c_0$. The speculation is supported by the shape of the E/Nk_BT vs. c_{-}^{1}, which becomes more flat and in the case of $c_0 = 0.5$ M even starts to decrease for $c_{-}^{1} > c_0$. A decrease in the absolute value of the energy for $c_{-}^{1} < c_0$ indicates that it is not energetically favourable for an invading electrolyte to find itself in the quenched environment (see also Figure 3).

Due to the correlations between fluid and matrix ions, the fluctuations of the electrolyte ions are suppressed, and at high electrolyte concentrations the compressibility of the annealed electrolyte (Figure 2c) decreases with the increasing concentration of matrix ions. At low electrolyte concentrations just the opposite is true.

The study of the adsorption (rejection) of the electrolyte in charged matrices was the main goal of this work. The Donnan exclusion coefficient, Γ, defined by equation 1 was calculated for all the examples shown above in Figure 2; the results are displayed in Figure 3. Here again (from top to bottom), the dash-dotted line and open squares correspond to $c_0 = 2.0$ M; the dotted line and filled squares to $c_0 = 1.0$ M; the dashed line and open circles to $c_0 = 0.5$ M, and the continuous line and filled circles to $c_0 = 0.05$ M charged matrix ($z_{-}^{0} = -1$).

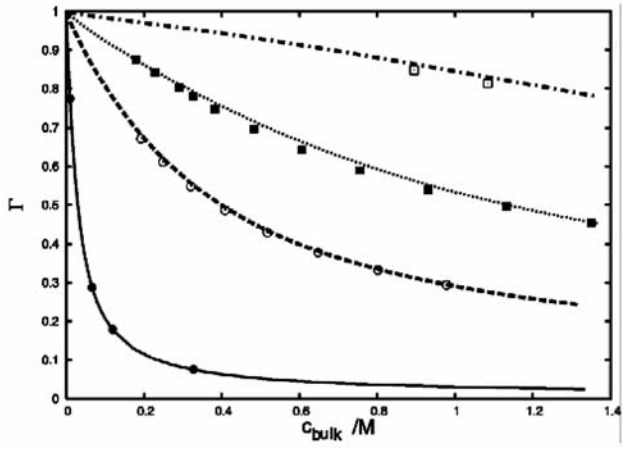

Figure 3: The Donnan exclusion coefficient, Γ, as a function of the bulk electrolyte concentration for various densities of charged matrices ($z_{-}^{0} = -1$). Lines denote the ROZ/HNC results, and symbols the GCMC simulations. Notation is as for Figure 2 – from top to bottom: $c_0 = 2.0$, 1.0, 0.5, and 0.05 M. In all the cases $\lambda_{B,0} = \lambda_{B,1} = 7.14$ Å.

According to the definition given by the equation 1, Γ approaches zero when there is no rejection (or adsorption), and assumes the value one in case of extreme rejection. In case of the net adsorption the Γ values should be negative. In all the cases shown here the electrolyte is to a smaller or larger extent excluded from the matrix (Γ > 0). We can explain this in the following way: under the influence of the negative matrix potential the coions are forced to leave the matrix, followed by some counterions to satisfy the electroneutrality condition. Such a mean-field type of explanation, which follows from the Poisson-Boltzmann and similar theories,[2] may not be valid for highly coupled systems containing trivalent ions as demonstrated by one of us.[34] At higher concentrations of the electrolyte present in the system, the exclusion is weaker (smaller value of Γ), which is a consequence of the stronger screening by the Coulomb forces. As expected, the exclusion coefficient is lower for smaller concentration of matrix ions (keeping their valence constant); in other words, smaller matrix charge density leads to a smaller electrolyte rejection. In none of the cases studied here the sorption of the electrolyte in the matrix was observed; in other words Γ was never negative. More complex relation between the Donnan coefficient and c_{bulk} has been found in case of the electroneutral matrices studied recently.[24]

In all the examples described above we varied the matrix charge density by changing its concentration. At the same time we were also changing the matrix packing fraction so the effects described are the result of the electrostatic forces and the excluded volume effect, combined. In an attempt to separate the two effects, we further studied the influence of the matrix charge on the electrolyte exclusion by changing the charge on the frozen matrix ions, fixing matrix concentration to c_0 at 0.05 M. The charge of the matrix ions was (see Figures 4 and 5) either zero, $z_-^0 = 0$ (dash-dotted line and open squares, $c_0 = 0.1$ M), $z_-^0 = -1$ (continuous line, filled circles), –2 (dashed line, open circles), –3 (dotted line, filled squares), and –4 (space-dotted line). The results for the thermodynamic properties are shown in Figure 4; the panel a) presents the mean activity coefficient, panel b) the excess internal energy, and panel c) the isothermal compressibility, all given as functions of the electrolyte concentration, c_-^1. In all the panels the data from bottom to top apply for $z_-^0 = -4, -3, -2, -1, 0$.

The charge density of the matrix, the values used here are: $\rho_e = 0$, -0.482×10^4, -0.965×10^4, -1.45×10^4, and -1.93×10^4 As dm^{-3}, for $z_-^0 = 0, -1, -2, -3$, and –4, respectively, influences the thermodynamics of the annealed electrolyte as shown in Figure 4. The Coulomb effects are more pronounced at low annealed electrolyte concentrations, while at high concentrations the differences in the thermodynamic properties are mostly due to the excluded volume effects. For high matrix charge densities and low electrolyte concentrations, the concentration fluctuations of the annealed electrolyte are suppressed due to the strong correlation with the matrix ions. As a consequence the isothermal compressibility (Figure 4c) decreases with the increasing matrix charge. Altogether, the conclusions are similar as arrived at on the basis of Figure 2 discussed previously.

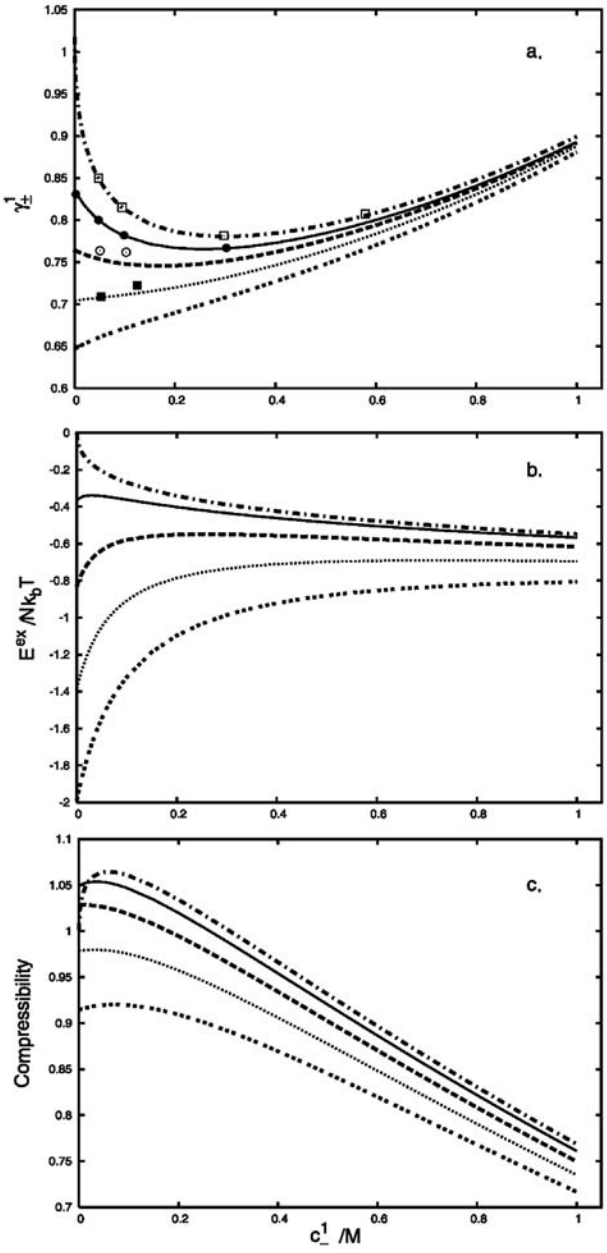

Figure 4: Thermodynamic quantities as a function of the annealed electrolyte concentration for various matrix charge densities. Lines denote the ROZ/HNC results, and the symbols the GCMC data. **a**) the mean activity coefficient. From top to bottom: (*i*) uncharged hard sphere matrix ($z^0 = 0$) – dash-dotted line, open squares; (*ii*) charged matrix ($z_-^0 = -1$) – continuous line, full circles; (*iii*) charged matrix ($z_-^0 = -2$) – dashed line, open circles; (*iv*) charged matrix ($z_-^0 = -3$) – dotted line, full squares; (*v*) charged matrix ($z_-^0 = -4$) – space-dashed line. **b**) The excess internal energy: labelled as on panel *a* (simulation results are not shown). **c**) The isothermal compressibility: labelled as on panel *a* (simulation results are not shown). For charged matrices, $\lambda_{B,0} = 7.14$ Å, and $c_0 = 0.05$ M. For the uncharged hard sphere matrix, $c_0 = 0.1$ M. In all the cases $\lambda_{B,1} = 7.14$ Å.

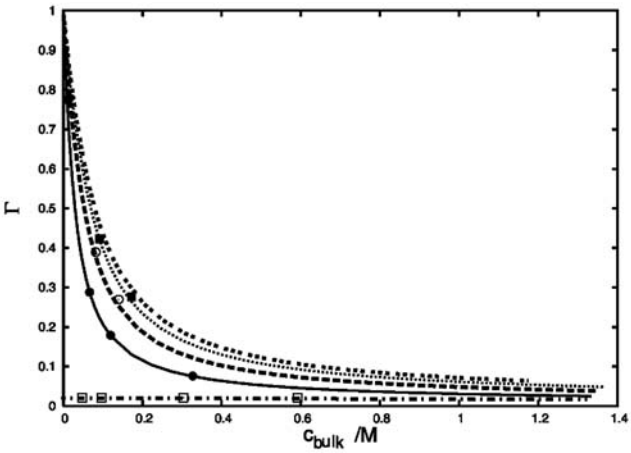

Figure 5: The Donnan exclusion coefficient, Γ, as a function of the bulk electrolyte concentration for various matrix charge densities. Lines denote the ROZ/HNC results, while symbols apply to the GCMC simulation. Notation used is the same as on Figure 4 (from top to bottom: z_0 = –4, –3, –2, –1 and 0). For charged matrices, $\lambda_{B,0}$ = 7.14 Å, and c_0 = 0.05 M. For the uncharged hard sphere matrix, c_0 = 0.1 M. In all the cases $\lambda_{B,1}$ = 7.14 Å.

The Donnan exclusion coefficients, calculated for matrices with different charge density (see Figure 5), differ substantially only at low concentrations of the external electrolyte. At higher electrolyte concentrations the matrix charges seem to be efficiently screened, and the charged matrix behaves essentially as an uncharged one. Note that Γ remains constant in the case of adsorption in the uncharged hard sphere matrix (Figure 5, dash-dotted line, open squares) for all values of c_{bulk} studied here.

It is of some interest to compare the results for the electrolyte adsorption in random charged matrices with adsorption in an array of charged cylindrical micropores.[2,3] For this purpose we in Figure 6 re-plotted our results for the Donnan exclusion coefficient, this time given as a function of $|z_-^0|$, which is at fixed concentration of obstacles, proportional to the matrix charge density. The concentration of the external electrolyte was kept constant at c_{bulk} = 0.1 M. The symbols represent the ROZ-HNC results, and the lines are used here merely to guide the eye.

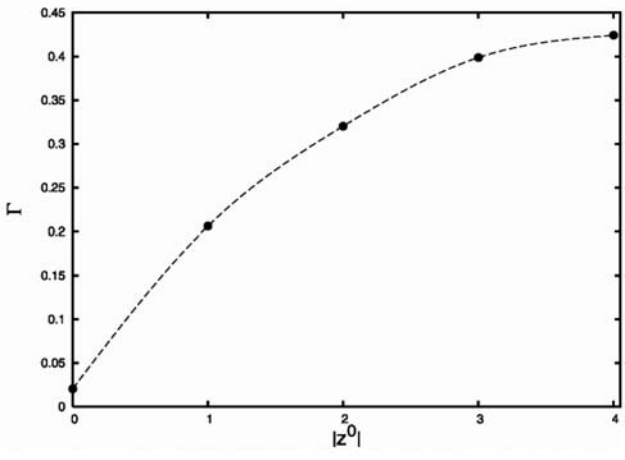

Figure 6: The Donnan exclusion coefficient, Γ, as a function $|z_-^0|$, for c_{bulk} = 0.1 M. Symbols show the the ROZ/HNC results, the dashed line is the smoothed fit through the points. For the charged matrices, $\lambda_{B,0}$ = 7.14 Å, c_0 = 0.05 M. For the uncharged hard sphere matrix ($|z^0|$ = 0), c_0 = 0.1 M. In all the cases $\lambda_{B,1}$ = 7.14 Å.

Although no quantitative comparison is possible we can say that the results obtained by two models (see also Figure 8 in Ref. 2) are similar. Strong repulsive interactions between the co-ions and matrix charges cause for the electrolyte to be excluded from the adsorbent. The fact that the same trend was observed in studies of absorption in an array of charged cylindrical micropores[2,3] suggests, that actual geometry of the micropores may be less important than the value of the charge density of the microporous material.

4. Conclusions

Thermodynamic properties of the +1 : –1 primitive model electrolyte, adsorbed on charged obstacles were examined, using the recently modified ROZ theory supplemented by the HNC approximation. To complete the picture, selected results for the adsorption in electroneutral ionic matrix, and in uncharged hard sphere matrix were also shown. Changes in thermodynamic properties of the adsorbed electrolyte, brought about by the presence of the matrix, depend on the concentration and charge of the obstacles forming the matrix, as well as on the concentration of the invading electrolyte. At high concentrations of the invading electrolyte, the adsorption is mostly dominated by the excluded volume effect. At low electrolyte concentrations, the behaviour of the model system is determined by the matrix charge density and the excluded volume effect combined. Similar effects, in general agreement with the experimental observations, were previously observed for the electrolyte absorbed in array of charged cylindrical micropores. Good agreement between the ROZ and Grand Canonical Monte Carlo results indicates usefulness of the ROZ theory in situations where the information about the distribution of particles forming the porous phase is provided in form of the pair distribution function or the structure factor. The ROZ/HNC theory is, namely, considerably less time consuming to use than the GCMC or any other computer simulation method.

5. Acknowledgment

The authors appreciate the financial support of the Ministry of Science and Education of Slovenia under grants P1-0201 and J1-6553. M. L. acknowledges partial financial support from *Ad futura* (Science and Education Foundation of the Republic of Slovenia). Part of the paper was written while V. V. was Visiting Professor at Ionic

Liquids & Charged Interfaces Laboratory at University of Pierre et Marie Curie (Paris 6), France; generous support of this institution is gratefully acknowledged.

6. References

1. F. Helfferich in: Ion Exchange, McGraw-Hill, New York, **1962**.
2. V. Vlachy, A. D. J. Haymet, *J. Electroanal. Chem.* **1990**, *283*, 77–85.
3. B. Jamnik, V. Vlachy, *J. Am. Chem. Soc.* **1993**, *115*, 660–666.
4. O. Pizio, S. Sokolowski, *J. Phys. Stud.* **1998**, *2*, 296–321.
5. A. Trokhymchuk, D. Henderson, A. Nikolov, D. T. Wasan, *J. Phys. Chem. B* **2003**, *107*, 3927–3937.
6. D. Henderson, A. Trokhymchuk, A. Nikolov, D. T. Wasan, *Ind. Eng. Chem. Res.* **2005**, *44*, 1175–1180.
7. F. Donnan, *Z. Elektrochem.* **1911**, *17*, 572–581.
8. W. G. Madden, E. G. Glandt, *J. Stat. Phys.* **1988**, *51*, 537–558.
9. W. G. Madden, *J. Chem. Phys.* **1992**, *96*, 5422–5432.
10. J. A. Given, G. Stell, *J. Chem. Phys.* **1992**, *97*, 4573–4574.
11. J. A. Given, G. Stell, *Physica A* **1994**, *209*, 495–510.
12. J. A. Given, *J. Chem. Phys.* **1995**, *102*, 2934–2945.
13. H. Tatlipinar, G. Pastore, M. P. Tosi, *Phil. Mag. Lett.* **1993**, *68*, 357–361.
14. M. L. Rosinberg, G. Tarjus, G. Stell, *J. Chem. Phys.* **1994**, *100*, 5172–5177.
15. M. L. Rosinberg, in: C. Caccamo, J. P. Hansen, G. Stell (Eds.): New Approaches to Problems in Liquid State Theory, Kluwer, Dordrecht, **1999**, pp 245–278.
16. O. Pizio, in: M. Borowko (Ed.): Computational Methods in Surface and Colloid Science, Marcel Dekker, New York, **2000**, pp 293–345.
17. B. Hribar, O. Pizio, A. Trokhymchuk, V. Vlachy, *J. Chem. Phys.* **1997**, *107*, 6335–6341.
18. B. Hribar, O. Pizio, A. Trokhymchuk, V. Vlachy, *J. Chem. Phys.* **1998**, *109*, 2480–2489.
19. B. Hribar, V. Vlachy, O. Pizio, *J. Phys. Chem. B* **2000**, *104*, 4479–4488.
20. B. Hribar, V. Vlachy, O. Pizio, *J. Phys. Chem. B* **2001**, *105*, 4727–4734.
21. B. Hribar, V. Vlachy, O. Pizio, *Mol. Phys.* **2002**, *100*, 3093–3103.
22. H. Dominguez, B. Hribar, V. Vlachy, O. Pizio, *Physica A* **2003**, *424*, 471–483.
23. V. Vlachy, H. Dominguez, O. Pizio, *J. Phys. Chem. B* **2004**, *108*, 1046–1055.
24. M. Lukšič, V. Vlachy, O. Pizio, *Acta Chim. Slov.* **2006**, *53*, 292–305.
25. M. Lukšič, B. Hribar-Lee, V. Vlachy *J. Phys. Chem. B* **2007**, *111*, 5966–5975.
26. P. R. Van Tassel, J. Talbot, P. Viot, G. Tarjus, *Phys. Rev. E* **1997**, *56*, R1299–R1301.
27. P. R. Van Tassel, *Phys. Rev. E* **1999**, *60*, R25–R28.
28. L. Zhang, P. R. Van Tassel, *J. Chem. Phys.* **2000**, *112*, 3006–3013.
29. L. Sarkisov, P. R. Van Tassel, *J. Chem. Phys.* **2005**, *123*, 164706–164715.
30. L. Zhang, P. R. Van Tassel, *Mol. Phys.* **2000**, *98*, 1521–1527.
31. L. Zhang, S. Cheng, P. R. Van Tassel, *Phys. Rev. E* **2001**, *64*, 042101–042104.
32. D. Frenkel, B. Smith in: Understanding molecular simulation: from algorithms to applications, Academic Press, San Diego, **2002**, pp. 126–135.
33. V. Vlachy, T. Ichiye, A. D. J. Haymet, *J. Am. Chem. Soc.* **1991**, *113*, 1077–1082.
34. V. Vlachy, *Langmuir* **2001**, *17*, 399–402.

Povzetek

V članku smo z uporabo "Replica" Ornstein-Zernikove teorije in računalniške simulacije Monte Carlo študirali adsorpcijo simetričnega +1 : –1 elektrolita v neurejeni porozni snovi. Adsorbent smo pripravili z nenadno zamrznitvijo pri temperaturi T_0 in dielektrični konstanti ε_0 uravnoteženega + 1 : z_-^0 (z_-^0 = –1, –2, –3, in –4) elektrolita. Pri tem so ostali zamrznjeni le negativni ioni, pozitivni pa so se, skupaj z adsorbiranim +1 : –1 elektrolitom, pri temperaturi T in dielektrični konstanti ε_1 prosto gibali v adsorbentu. Rezultate smo primerjali z adsorpcijo enakega +1 : –1 elektrolita v elektronevtralnem adsorbentu (zamrznjeni so ostali tako anioni kot kationi adsorbenta) in adsorbentu brez nabojev (sestavljen iz nenabitih togih kroglic). Pri raziskavi so nas še posebej zanimale termodinamične lastnosti adsorbata, kot so srednji aktivnostni koeficient in Donnanski izključitveni koeficient, v odvisnosti od naboja in koncentracije delcev adsorbenta. Rezultati kažejo, da je adsorpcija pri višjih koncentracijah adsorbata določena predvsem s steričnimi vplivi, pri nižjih pa jo določa kombinacija obeh vplivov; to je, izključitvenega volumna in vpliva gostote neto naboja adsorbenta. Te ugotovitve se kvalitativno ujemajo s tistimi, dobljenimi za adsorpcijo elektrolita v nabitih cilindričnih mikroporah.